PERGAMON

International Journal of Heat and Mass Transfer 42 (1999) 3361–3371

International Journal of HEAT and MASS TRANSFER

Shape and topology design for heat conduction by Evolutionary Structural Optimization

Qing Li[a], Grant P. Steven[a,*], Osvaldo M. Querin[a], Y.M. Xie[b]

[a]*Department of Aeronautical Engineering, Engineering Faculty, The University of Sydney, Sydney, NSW 2006, Australia*
[b]*Faculty of Engineering and Science, Victoria University of Technology, P.O. Box 14428, MCMC, Melbourne, Victoria 8001, Australia*

Received 24 July 1998

Abstract

This paper extends the algorithm of Evolutionary Structural Optimization to shape and topology design problems subjected to steady heat conduction. This extension incorporates an evolutionary iterative process into finite element heat solutions. During each iteration two basic steps are involved. Firstly, a finite element thermal solution is carried out for the current structure. Secondly, a small part of the material which cannot effectively contribute to the functionality of transferring heat is removed. Examples demonstrate the proposed evolutionary procedure being effective in solving heat conduction problems, which conventionally require sophisticated mathematical programming techniques. © 1999 Elsevier Science Ltd. All rights reserved.

Keywords: Shape and topology optimization; Evolutionary Structural Optimization; Heat conduction; Finite element analysis

1. Introduction

In recent years, a great deal of effort has been devoted to the development of various numerical techniques for solving thermal issues. Finite element analysis (FEA) has become a widely used tool for engineers of many disciplines. Relatively speaking, the inverse design problems have achieved far less popularity in practice compared with the finite element analysis itself. In these types of problems, shape and topology optimization of thermal structure may be regarded as a significant aspect.

Most of the research on shape and topology optimization has focused on elasticity problems [1–3]. The thermal conducting solid issue has received relatively less attention in spite of its significance. Cooling fins, thermal diffusers and moulding dies are examples of shape optimization in this category [4]. Recently, the shape design sensitivity analysis (SDSA) has played a crucial role in solving shape optimization problems subject to heat transfer process, as reviewed by Kwak [5]. This has been developed by a number of researchers since the 1980's. Haftka [6] presented the finite element based technique for computing the sensitivity of temperatures with respect to the changes in design variables. Later, Park and Yoo [7] developed the boundary element based algorithm for the SDSA. Dems [8] and Tortorelli et al. [9] derived the sensitivity formulations for linear and non-linear thermal systems by using the Lagrangian multiplier technique and adjoint variable method. Meric [10,11] presented the

* Corresponding author. Tel.: +61-2-9351-2183; fax: +61-2-9351-4841.

E-mail address: grant@aero.usyd.edu.au (G.P. Steven)

0017-9310/99/$ - see front matter
PII: S0017-9310(99)00008-3

Nomenclature

ER	evolution rate
f_x, f_y, f_z	heat flux components in x, y, z directions
f_{RMS}, f^{e}_{RMS}	magnitude of the element flux
$\tilde{f}^{e}_{RMS}, \hat{f}^{i}_{RMS}$	smoothed elemental and nodal flux
J	integral of structural temperature or flux
J^{e}	integral of element e
J^{max}	maximum integral of all elements
$J^{e}_{RMS}, J^{e}_{x}, J^{e}_{y}, J^{e}_{z}$	integrals of elemental flux
K_x, K_y	coefficients of conductivity in x, y direction
M	number of elements
N	number of heat sources or heat load cases
RR_i	rejection ratio at the ith steady state
RR_0	initial rejection ratio
SS	number of ESO Steady State
T	temperature
V	volume of current structure
V_0	volume of initial design model.

SDSA expressions for optimization of heat conducting solid bodies. Saigal and Chandra's work [12] linked the heat transfer and sensitivity analysis to a numerical optimization algorithm. In the above approaches, one common point is to optimize the structure shape by changing nodal coordinates. Although these SDSA based methods attempted to represent the geometry of a complex model in a very efficient manner, the boundary shape has to be restricted by the design variables and boundary functions, and a sophisticated re-meshing process is often required after each iteration. The mathematical complexity and computational cost sometimes becomes prohibitive in practical problems.

Recently, significant progress has been made in trying to avoid re-meshing or altering nodal position [1–3]. The basic idea of the technique aims at finding unnecessary or inefficient portions of a structure and eliminating them from the FEA model. There are two popular approaches: (1) Continuous design variable methods, e.g. 'Homogenization method' [1], where relative densities (0–1) of elements are treated as design variables; and (2) 'Discrete design variable methods', where the binary (0 or 1) decision-making algorithm is employed to remove the unnecessary material, e.g. the Simulated Annealing (SA) method [13] and the Evolutionary Structural Optimization (ESO) method [2,14–16]. In general, the former needs to involve the complicated sensitivity analysis and mathematical programming, while the latter takes advantage of powerful computing technology thereby having a much simpler formulation.

The Evolutionary Structural Optimization method developed by Xie and Steven in 1993 [14] has demonstrated the capabilities of dealing with various mechanical issues [2,14–16]. Considering the analogy in many aspects between thermal and structural FEA, an attempt is therefore made to extend the ESO method to shape and topology optimization of thermal problems. The numerical experiments presented in this paper show that this algorithm is no longer necessary to perform the tedious calculus and variational operations, nor to undertake complicated mathematical programming. Moreover, the ESO method is able to flexibly handle various optimal objectives by simply selecting the appropriate rejection criterion, e.g. temperature or heat flux. In practice, the algorithm can be easily integrated with current commercial finite element heat analysis packages, hence showing strong application prospects.

2. Optimality criteria for thermal problems

For thermal conduction, a region is expected to seek as close to an even distribution of temperature or heat flux as possible on the design domain. In order to evaluate the performance of a resulting shape or topology subjected to the steady heat conduction, the optimization criterion can be described by averaging the domain integral [11]:

$$J = \frac{1}{V} \int_V T \, \mathrm{d}V \tag{1}$$

Sometimes, the optimization may also be subject to a volume constraint as [11]:

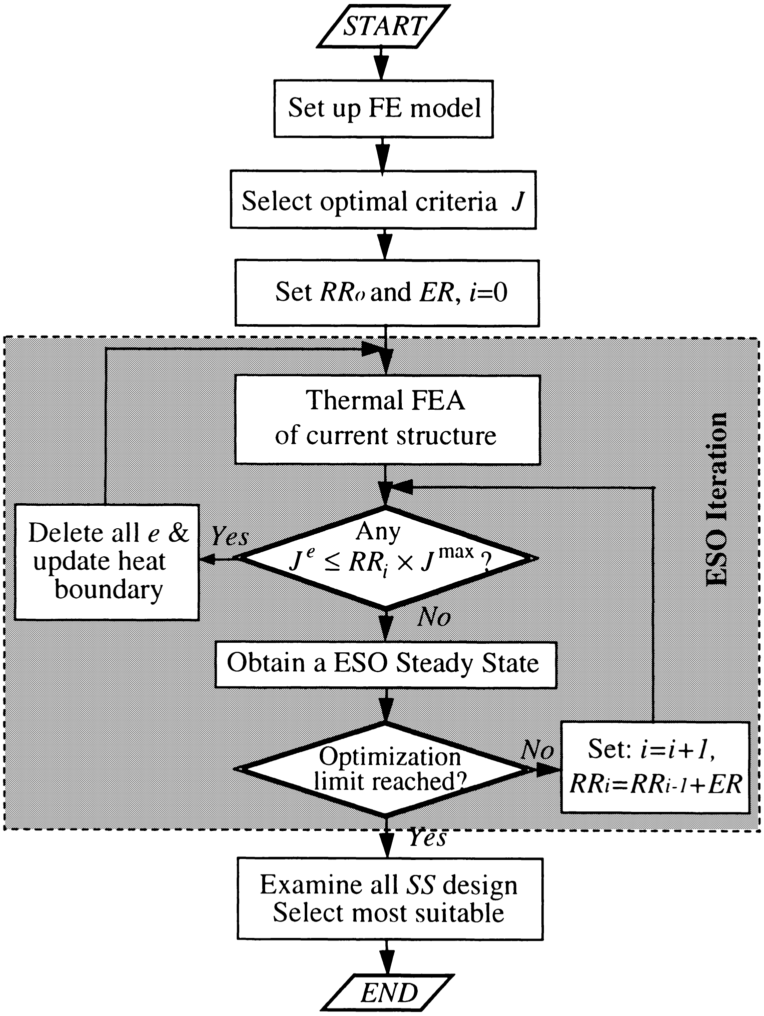

Fig. 1. Flow chart of the ESO procedure.

$$\int_V \mathrm{d}V - V_\mathrm{p} \geq 0 \tag{2}$$

where V_p is the prescribed material volume.

In finite element analysis, the overall thermal performance of a region can be decided in terms of each element's contribution. The integral over the design domain can be broken into individual one in each element. Consequently, the integral of different thermal parameters over the element, J^e, could be taken as a criterion of elemental thermal performance, i.e.

$$J^\mathrm{e} = \frac{1}{V_\mathrm{e}} \int_{V_\mathrm{e}} T^\mathrm{e} \, \mathrm{d}V_\mathrm{e} \tag{3}$$

Here parameter T^e might be either the temperature or the heat flux distribution over an element. The integrals of different flux components can be denoted by:

$$J_x^\mathrm{e} = \frac{1}{V_\mathrm{e}} \int_{V_\mathrm{e}} |f_x| \, \mathrm{d}V_\mathrm{e}$$

$$J_y^\mathrm{e} = \frac{1}{V_\mathrm{e}} \int_{V_\mathrm{e}} |f_y| \, \mathrm{d}V_\mathrm{e}$$

$$J_z^\mathrm{e} = \frac{1}{V_\mathrm{e}} \int_{V_\mathrm{e}} |f_z| \, \mathrm{d}V_\mathrm{e} \tag{4}$$

where J_x^e, J_y^e and J_z^e are respectively the element integrals of flux components in x. y, z directions. Usually, the magnitude f_{RMS} of the elemental heat flux vector is used to define the optimality criterion:

$$J^{\mathrm{e}}_{RMS} = \frac{1}{V_{\mathrm{e}}}\int_{V_{\mathrm{e}}} f_{RMS}\,\mathrm{d}V_{\mathrm{e}} \tag{5}$$

where $f_{RMS} = \sqrt{f_x^2 + f_y^2 + f_z^2}$.

In fact, the integrals J^{e} and J^{e}_{RMS} indicate the average of temperature or heat flux over the element material. They may be viewed as the thermal performance and contribution of a candidate element. From the standpoint of material efficiency, an optimum design could be expected to have the temperature or flux distribution over the structure as even as possible. In the case of *shape design*, the elements only on specified boundaries are regarded as the design domain and are available for removal during the evolutionary process. The integrals for all these elements should be close to an equal level, thus approach each an *iso-thermal* or *iso-fluxed* element. In the case of *topology design*, all elements in the specified regions are considered as the design domain. The integral levels of all remaining elements may not be close to an equal level, but are expected to become more uniform as the evolutionary process develops, thereby the term *fully-fluxed* could be used.

3. Evolutionary Structural Optimization (ESO) for heat conduction

The temperature or heat flux distribution throughout a specified structure can be found by finite element thermal analysis. It often happens that not all material is effectively utilized. In other words, the element integrals (J^{e}) in some material regions may be distinctly smaller than those of others. This means the material of the former is not making a significant contribution to the thermal performance of the region. If the region is divided into a fine mesh of finite elements, the removal of material from the structure can be conveniently represented by removing elements from the finite element model. To do so, the ESO algorithm introduces a concept of *rejection criteria* (RC), by which those under-utilized elements in the region will be removed. For example, if some elements' integral levels J^{e} are less than a *rejection ratio* (RR_i) times the highest one among all the elements of the design domain, i.e.

$$J^{\mathrm{e}} \le RR_i \times J^{\max} \tag{6}$$

these elements will be eliminated from the structure. Such a thermal FEA and element elimination cycle is repeated using the same RR_i, until an ESO *Steady State* (SS) is reached. This means that there are no more elements that can be removed at the current RR_i. As a result, the lowest level of $T^{\min}$ or $f^{\min}_{RMS}$ in the structure has been higher than a specified level (i.e. RR_i times maximum value at least).

When an ESO Steady State is reached, an *evolution rate* (ER) is introduced and added to the rejection ratio ($RR_{i+1} = RR_i + ER$). The iterations take place again until a new ESO steady state is attained. The *evolution rate ER* is used as an increment of the rejection ratio (RR_i) so that the elimination criterion of elements is increased to a higher level. If the ER is set sufficiently small, the number of elements removed between two ESO Steady States can be controlled within a small value. The procedure is described in detail using the flow chart shown in Fig. 1.

It must be pointed out that the evolution rate (ER) should be selected to be reasonably small (for example between 0.1% and 1%, refer to [2]). This is because, in many circumstances, the thermal boundary condition (e.g. prescribed boundary temperature or flux) needs to gradually migrate with the elimination of the elements. In order to avoid a big leap in the change of both boundary conditions and the structural thermal responses, the number of elements removed at each stage should not be too great.

4. Implementation of the ESO method

The ESO method is based on the simple concept that by slowly removing inefficient material from a structure, the resulting region evolves towards an optimum. The material elimination can occur in any part of a structure as long as the flux level or other objective integral as in Eqs. (1)–(3) in that part is relatively low compared to the maximum or the mean. This allows internal cavities being created and new topologies being generated, and is, conventionally, called topology optimization. In other cases, internal cavities are not allowed and the structure can be modified at the boundaries, which is traditionally classified as shape optimization problems. Moreover in reality, some structures are required to operate under the cases of multiple thermal loads or heat sources. The appropriate schemes need to be developed for dealing with different heat load cases. The implementation of above features of the thermal criterion-based ESO method is discussed below.

4.1. ESO for shape optimization

For shape optimization, not the whole structure but only the specified boundaries of the structure are of interest. In the ESO method, this is called *nibbling* [2]. The algorithm of nibbling ESO is that an element satisfied the elimination criterion can be removed if at least one of its edges or sides is not connected to any other elements in the structure. The nibbling constraint allows the ESO method to behave in a similar manner to shape optimization, by only altering the surrounding shape/perimeter of a structure.

In some cases, the thermal boundary conditions, e.g. temperature and/or heat flux, also need to be migrated with the change of structural boundary. This can be implemented by imposing a new thermal boundary to those elements connected to the ones being eliminated in the current iteration.

4.2. ESO for topology optimization

As mentioned before, internal cavities are allowed in this case, in for which the relative level of flux is the unique criterion for element rejection. If an *iso-flux* boundary is deemed as the objective of shape design, the as *even* as possible distribution of flux is the goal of topology optimization. After the lowly fluxed material is gradually removed, the flux levels in the remaining material are larger than a certain percentage value of the highest level. This means that a more fully fluxed design has been achieved and the material is used more efficiently in both structural and thermal sense.

The checkerboard patterns, as discussed in [1] for topology optimization of mechanical problems, can also be observed in heat conduction problems based on the ESO procedure. Indeed, the checkerboarding phenomenon is quite typical in almost all finite element based topology optimization methods and therefore suppression schemes have to be employed [1]. In the flux based ESO procedure, a simple local smoothing technique of element reference integral is used by: (1) calculating the reference integral $\hat{J}^i$ at each node by averaging the values of elements connecting to this node; $\hat{J} = \sum_{e=1}^{C_i} J^e$; and then (2) calculating the smoothed reference integral $\tilde{J}^e$ of the specific element by averaging the nodal reference integrals of this element, $\tilde{J}^e = \sum_{i=1}^{4} \hat{J}^i$. Consequently, the smoothed element integral $\tilde{J}^e$ is used as the evolutionary criterion for dealing with the checkerboard issue.

4.3. ESO for multiple heat load cases

In multiple heat load cases, a number of heat sources may act on the structure at different times, locations and heat boundary conditions. It is worth noting that the separate effects of individual heat sources on the structure are quite different from the simultaneous ones of all heat sources. In general, there are two simple approaches to combining the evolutionary criteria in different heat load cases:

1. Logical AND Scheme, in which an element is eliminated from the structure only if the rejection criteria are satisfied by all load cases, i.e.

   Logical AND Scheme:

$$\begin{cases} \text{Load Case 1:} \quad J_1^e \le RR_i \times J_1^{\max} \\ \vdots \\ \text{Load Case } N\text{:} \quad J_N^e \le RR_i \times J_N^{\max} \end{cases} \tag{7}$$

   where $J_1^e, \ldots, J_N^e$ denote the elemental flux integrals under heat load case 1, ..., N respectively and N is the total number of heat load cases;
2. Weighting Factor Scheme, in which the relative contribution of an element to the structural thermal performance in one heat source is evaluated by the ratio of its reference integral to the corresponding maximum one under this load case ($\gamma_j = J_j^e/J_j^{\max}$), then add all the contributions of the different load cases by the weighting factors (w_j, $j = 1, 2, \ldots, N$), finally the elements with minimum overall contribution for all load cases are eliminated from the structure, i.e.

Weighting Factor Scheme:

$$\begin{cases} j^{\text{th}} \text{ Load Case: } \gamma_j = J_j^e/J_j^{\max} \ (j = 1, \ldots, N) \\ \tilde{F}^e = w_1 \times \gamma_1 + \cdots + w_N \times \gamma_N \\ \tilde{F}^e \le RR_i \times \tilde{F}^{\max} \end{cases} . \tag{8}$$

In the evolution process, the different schemes may yield quite different shapes or topologies. When the Logical AND Scheme is used, as in Eq. (7), the surviving elements have their own roles to play in at least one load case and possibly in all load cases. In this scheme, it is obvious that the best thermal performance of an element under different heat loading will determine its presence or absence. When using the Weighting Factor Scheme (Eq. (8)), the remaining elements in a structure are of a higher overall contribution to the thermal performance. According to different design requirements, an appropriate scheme needs to be chosen. In some situations, it may even be necessary to compare the results of using both the schemes.

5. Example illustrations

The following examples are used to demonstrate the capabilities of the proposed ESO procedure for solving shape and topology optimization problems subjected to steady heat conduction. The flux magnitude integral J_{RMS}^e, as given in Eq. (5), is used for the evolutionary optimality criterion in all following examples. For simplicity, all examples are modeled using two-dimensional four node quadrilateral elements with a unit

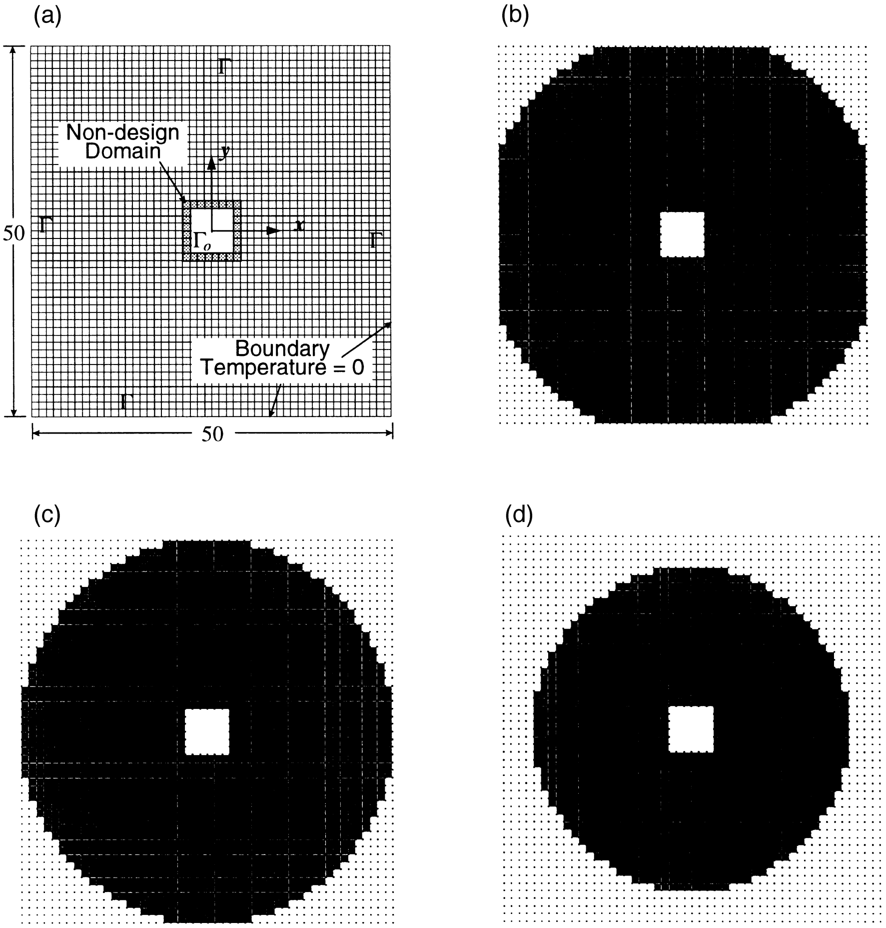

Fig. 2. Evolution history of shape optimization ($K_x = K_y = 1$, $T_{\Gamma_0} = 100°C$): (a) initial FEA model for the hollow solid: (b) Steady State 8, $V/V_0 = 88\%$; (c) Steady State 10, $V/V_0 = 79\%$ (form a circle); (d) Steady State 12, $V/V_0 = 55\%$.

thickness. In the evolution history pictures shown in the figures, the black areas represent the remaining elements and the small dots represent the nodes of the initial finite element model.

5.1. Shape optimization: outer boundary design of hollow solids

In this example, the outer boundary profiles are optimized for either isotropic or orthotropic material properties. The region is modeled using a 50×50 FE (finite element) mesh as shown in Fig. 2a). A square hole with dimensions of 6×6 is designed as the fixed inner boundary of the hollow solids. A layer of material adjacent to the inner hole is defined to be the non-design domain, where the elements cannot be removed during the evolution processes. In both cases below, the temperature at the four edges of the inner square hole is set at 100°C and the temperature at the outer boundary is always 0°C, regardless of positions.

The objective is to find an optimal outer profile so that the heat flux magnitude (f_{RMS}) of all boundary elements can be as evenly distributed as possible, i.e. *iso-fluxed*. In the evolution process, those elements with relatively low flux levels are gradually eliminated from the outer boundary, thereby the difference of flux levels is progressively reduced. The ESO driving parameters are set to the initial rejection ratio $RR = 1\%$ and the evolution rate $ER = 1\%$ for these two cases.

5.1.1. Case 1

For the region illustrated in Fig. 2(a), an isotropic conductive material is used (i.e. thermal conductivities $K_x = K_y$). Figs. 2(b)–(d) give the different stages of the evolution history. It can be seen that a circular outer boundary is gradually formed as shown in Fig. 2(c). The result is in good agreement with the hollow design problems in many references [17,18]. When further iterations are carried out in search of a new ESO steady state, it could be observed that this only results in a

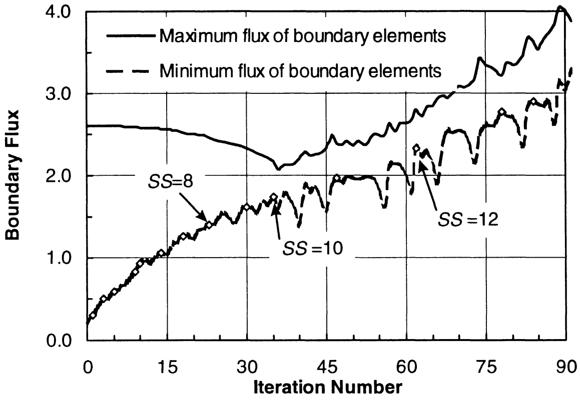

Fig. 3. Iteration history of the boundary flux integrals.

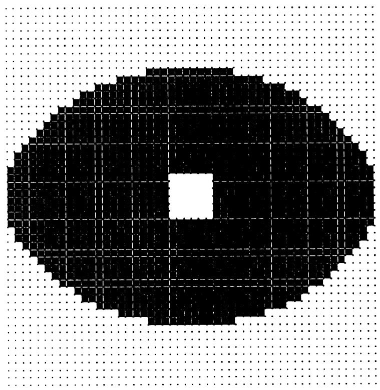

Fig. 5. Optimal shape of orthotropic conductivity (Steady State 11).

change in the size of the circle as shown in Figs. 2(c) and (d).

Shown in Figs. 3 and 4 are respectively the iteration and steady state histories of the maximum and minimum fluxes on the shaped outer boundary elements. It can be clearly seen from these two figures that the difference between the maximum and the minimum values is gradually reduced from the initial state to iteration 35 (corresponding to Steady State 10). At this stage (Iteration 35 and corresponding to $SS = 10$), a circular profile is formed. After that, the difference in the maximum and minimum fluxes on the shaped boundary remains almost unchanged, as shown in Fig. 4, consequently, a series of circular profiles with different sizes are yielded. Theoretically, the deviation between maximum and minimum should be close to zero for an *iso-fluxed* shape. However, for a fixed grid approach like ESO, it is hardly possible to obtain such a perfect iso-fluxed profile due to the approximation of the smooth boundary by a jagged profile and the imposition of the non-smooth thermal boundary. Consequently, a constant deviation has indicated a stable state for the shaped profiles. Besides, from Fig. 3 one can also find that a ESO Steady State always appears at a stage with the minimum difference among all iteration steps between two Steady States. This implies that each ESO Steady State can be an optimized solution.

5.1.2. Case 2

This case is similar to Case 1 except that the material has orthotropic conductivity, where the thermal conductivities in x and y direction are $K_x/K_y = 2$. It can be seen from Fig. 5 that an elliptic profile is produced as the evolution procedure progresses. The non-circular shape of the optimal outer boundary is the result of the anisotropic feature of the material. It is interpreted that the heat transfers *faster* in the x direction so that the material in this direction is of higher conducting efficiency.

Fig. 6 also shows a similar trend to that in Case 1. Before Steady State 11, the difference between maxi-

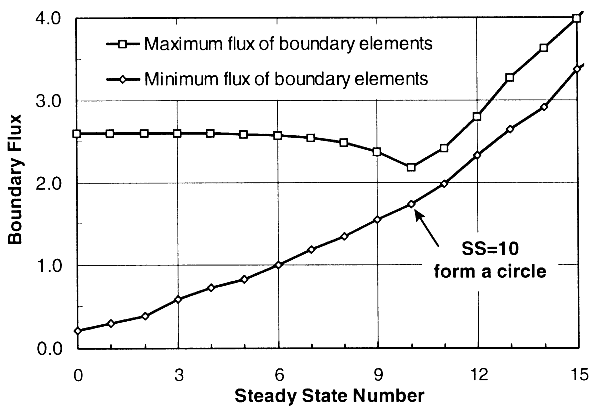

Fig. 4. Steady State history of the boundary flux integrals.

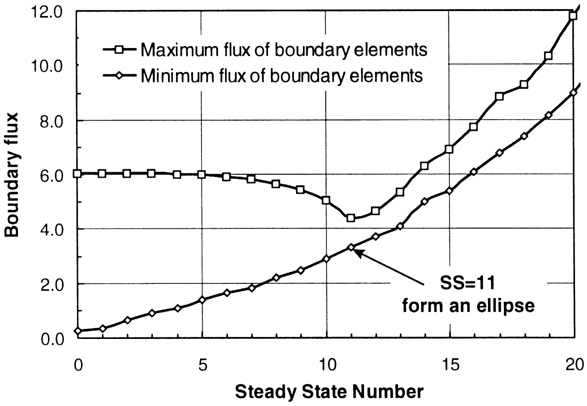

Fig. 6. Steady State history of the boundary flux for orthotropic conductivity.

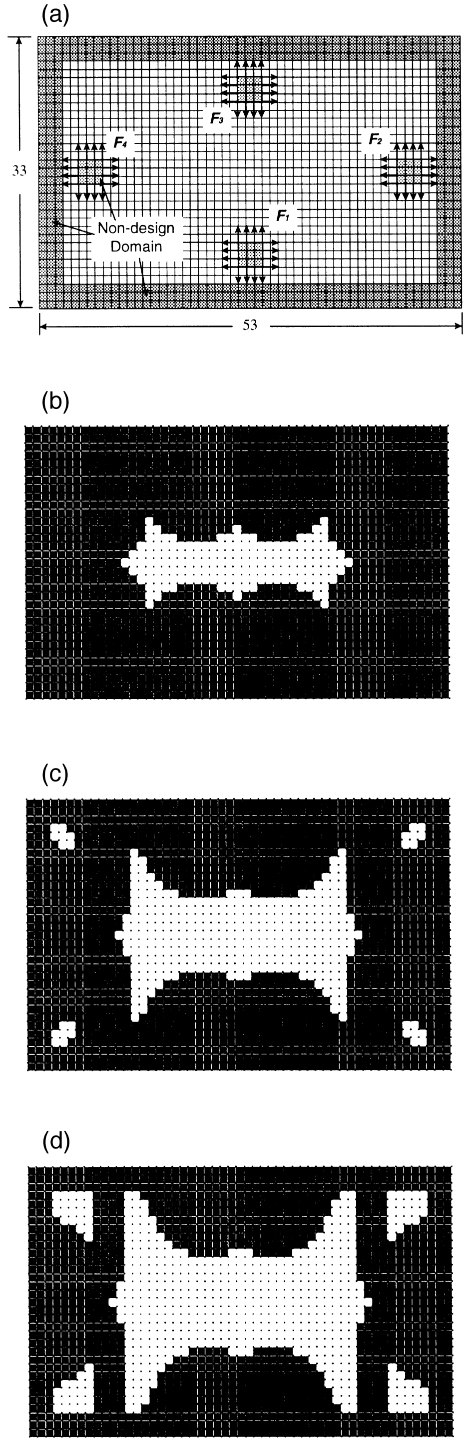

Fig. 7. Evolution history of flux based topology optimization for PCB substrate: (a) initial FEA model of the PCB substrate; (b) Steady State 32, $V/V_0 = 90\%$; (c) Steady State 48, $V/V_0 = 80\%$; (d) Steady State 57, $V/V_0 = 68\%$ (optimized).

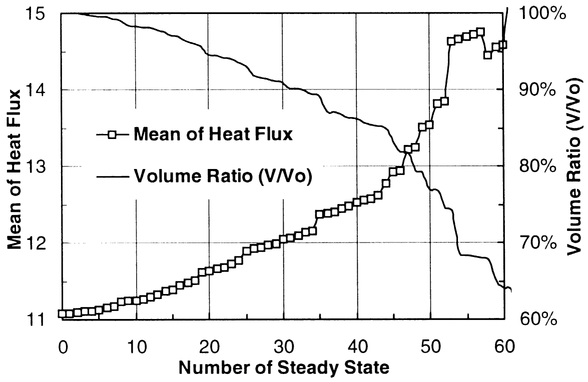

Fig. 8. Evolution histories of mean flux and volume ratio.

mum and minimum fluxes in the boundary gradually gets close as the evolution progresses. After $SS = 11$, there has been little change in the deviation. As a result, the ellipse shown in Fig. 5 has been a stable shape. More iterations only change the size of the ellipse but not its aspect ratio. This result is similar to that reported by Meric [11].

5.2. Topology optimization: printed circuit board (PCB) substrate design

This example intends to show the feature of topology optimization using the proposed evolutionary procedure. A printed circuit board (PCB) substrate subjected to steady heat conduction is considered. Previous work on PCB substrate topology optimization was based on an optimality criterion of the transient thermal stress and its gradient [19]. In practice, another functionality of a PCB substrate is to dissipate the highest amount of thermal energy with a limited amount of material. In accordance with the concept of optimizing material efficiency and thermal performance, a flux-based criterion is applied to this problem, in which elements with a relatively low flux level are gradually eliminated from the design domain. The removal of lowly fluxed material results in a more uniform flux distribution by reducing the flux variation in the structure.

As shown in Fig. 7(a), an FEA model of the PCB substrate is designed with a mesh of 53×33 elements. Four steady heat flux loading, F_1, F_2, F_3 and F_4, are set to 1 KW/m^2, which are generated by several major electronic components mounted on the PCB. The structure consists of design and non-design domains as illustrated in Fig. 7(a). The temperature on the outer boundary is maintained at 0°C throughout the evolution process. Maximizing the mean flux over the entire region is taken as the optimization objective and a volume ratio greater than 65% is prescribed for the constraint. The evolutionary parameters of the initial

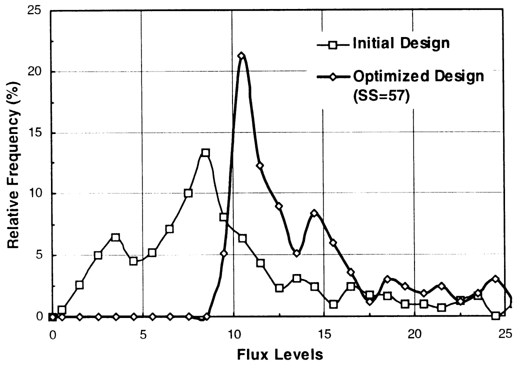

Fig. 9. Comparison of heat flux histograms of PCB design.

rejection ratio $RR_0 = 1\%$ and the evolution rate $ER = 1\%$ are set.

Figs. 7(b)–(d) display the evolutionary history of the PCB design at several different ESO Steady States and the corresponding volume ratios. The flux integral J_{RMS} is plotted in Fig. 8. Here a peak value occurs at Steady State 57 corresponding to Fig. 7(d). The improvement of thermal efficiency in a structure can also be observed by plotting the histograms of flux levels as Fig. 9. At initial state ($SS = 0$), only 35% material is fluxed between 10 and 25, whereas other 65% is lower than this range. When the structure evolves to Steady State 57, around 75% of material is fluxed in the same range. This is a significant improvement and means that a much more fully fluxed design has been achieved.

5.3. Optimization subjected to multiple heat load cases

The following examples are used to show the features of the proposed ESO combination schemes for solving the problems with multiple heat load cases.

5.3.1. Case 1: shape optimization under multiple heat sources

Two heat flux loading are applied to a rectangular plate with a dimension of 40×30 cm as illustrated in Fig. 10(a). The heat flux is input from either Source 1 or Source 2 at different times. The optimal design is to find a solution with the best compromise for both heat cases. In the ESO method, two different schemes are employed to deal with the optimal problems with multiple heat loads. For both the schemes (Logical AND and Weight Factor), the evolution parameters of an initial rejection ratio of 0.1% and an evolutionary rate of 0.1% are set.

The resulting shapes by using the Logical AND Scheme and Weighting Factor Scheme are shown in Figs. 10(b) and (c) respectively. It is interesting to note that the ESO solutions through different schemes produce the different profiles. In the Logical AND Scheme, the higher flux level of an element under both heat sources is taken as the reference value of its rejection criterion. Therefore the remaining material is

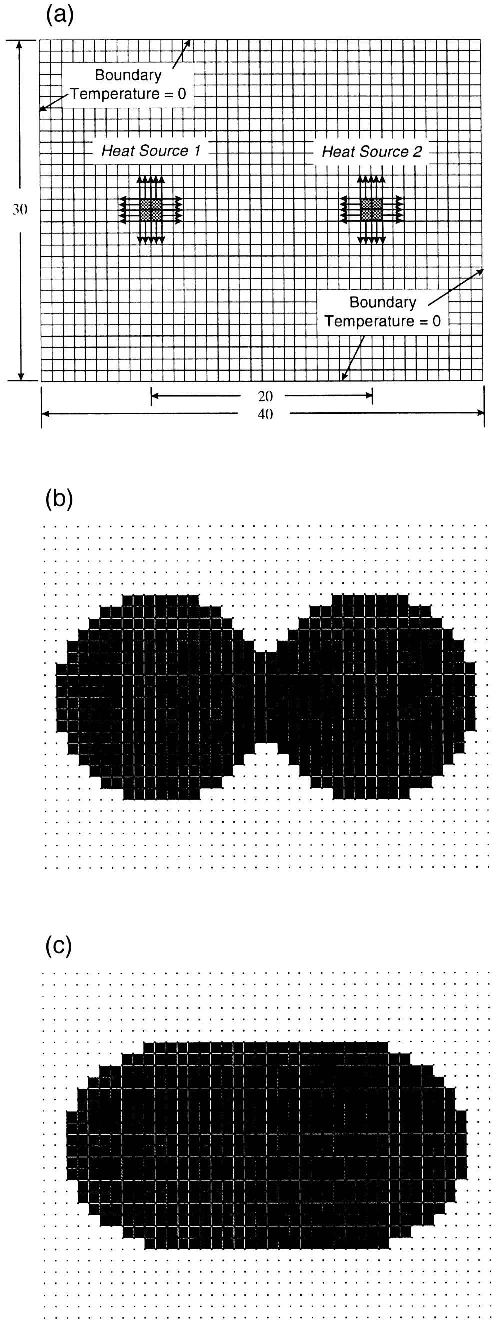

Fig. 10. Shape optimization subjected to multiple heat load cases: (a) initial FEA model under two heat flux loading; (b) resulting shape using Logical AND Scheme (Steady State 33, $V/V_0 = 46\%$); (c) resulting shape using Weighting Factor Scheme (Steady State 34, $V/V_0 = 47\%$).

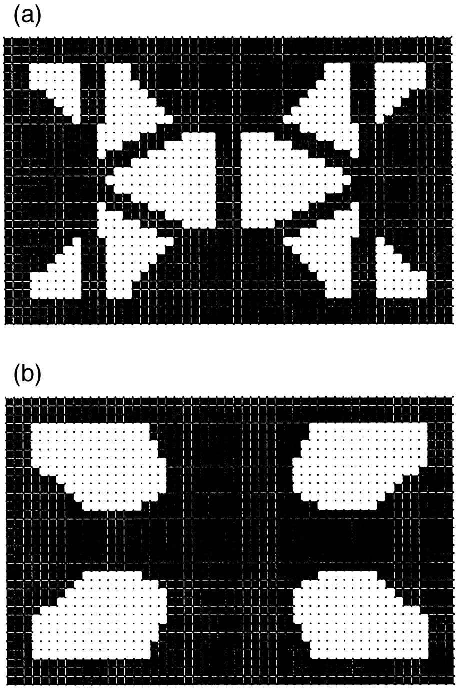

Fig. 11. Topology optimization for PCB substrate subjected to multiple heat load cases ($V/V_0 = 70\%$): (a) resulting topology using Logical AND Scheme; (b) resulting topology using Weighting Factor Scheme.

required by at least one of both heat sources. It can be seen that the resulting profile in Fig. 10(b) is shaped by joining two separate circular profiles. In the Weighting Factor Scheme, the reference value of an element is given in a combining manner by the weighting factors (here, $w_1 = w_2 = 0.5$). The rejection criterion of an element depends on its total contribution under both heat sources. As a result, the shaped profile as shown in Fig. 10(c) is of a uniform overall contribution rather than an individual one.

5.3.2. Case 2: topology optimization under multiple heat load cases

In the PCB substrate design of the previous example (as illustrated in Fig. 7(a)), those four heat sources are operated at the same time. In reality, it could also be the case that those differently located electronic components work at a different time.

The evolution parameters used in this example are the evolutionary rate $ER = 1\%$ and initial rejection ratio $RR_0 = 1\%$. Shown in Figs. 11(a) and (b) are the optimal topologies subjected to the same volume ratio constraint of 70% by using Logical AND Scheme and Weighting Factor Scheme respectively. The different resulting topologies further show the difference of two schemes in optimizing the thermal performance. By comparing Fig. 11(a) with Fig. 7(d), it can be found that there exists some topological resemblance between Logical AND combination scheme and the single heat load case except for the several truss-like connections in the PCB's central region. This shows that the Logical AND Scheme is focused more on the individual contribution of an element to each heat source. On the other hand, when using Weighting Factor Scheme (here: $w_1 = w_2 = w_3 = w_4 = 0.25$), the effect of one or two heat sources is often not enough to decide the presence and absence of an element. This scheme lays more emphasis on the overall contributions of an element to all heat load cases.

6. Concluding remarks

It can be concluded from this work that the shape and topology optimization in the presence of heat conduction can be easily solved by the proposed evolutionary procedure. Indeed, the shape or topology at each steady state may be chosen as an improved design. Thus it offers the designer with many sub-optimal solutions in the conceptual design stage. Usually, the designer can combine other factors such as structural efficiency, weight and manufacturing constraints to make a decision. For instance, when a volume constraint is imposed, the evolutionary shapes or topologies which satisfies the volume constraint may be considered as the final design.

The numerical experiments have shown that the thermal ESO procedure works simply and reliably for both shape and topology design, as well as for both single and multiple heat sources. In design, shape optimization evolves a structural boundary towards the *iso-fluxed* profile, whereas topology optimization evolves a structure towards the *fully-fluxed* layout or a more uniform flux distribution over the structure. In this study, two simple schemes, Logical AND and Weighting Factor, are presented to deal with the multiple heat loading problems.

In the structural optimization of thermal problems, further work can be to combine both flux based and thermal stress based criteria [16] into ESO procedure. The resulting shape or topology are expected to be of optimal mechanical and thermal performance. In addition, the work presented in this study demonstrates the possibility of extending the ESO procedure to other physical situations governed by the harmonic equation such as torsion, seepage, etc.

References

[1] M.P. Bendsøe, Optimization of Structural Topology, Shape, and Material, Springer-Verlag, Berlin, 1995.

[2] Y.M. Xie, G.P. Steven, Evolutionary Structural Optimization, Springer-Verlag, Berlin, 1997.
[3] G.I.N. Rozvany, M.P. Bendsøe, U. Kirsch, Layout optimization of structures, Applied Mechanics Review 48 (2) (1995) 41–118.
[4] B.Y. Lee, Shape sensitivity formulation for an axisymmetric thermal conducting solids, Proceedings of Institution of Mechanical Engineers Part C: Journal of Mechanical Engineering Science 207 (C3) (1993) 209–216.
[5] B.M. Kwak, A review on shape optimal design and sensitivity analysis, Structural Engineering/Earthquake Engineering 10 (1994) 159–174.
[6] R.T. Haftka, Techniques for thermal sensitivity analysis, International Journal for Numerical Methods in Engineering 17 (1981) 71–80.
[7] C.W. Park, Y.M. Yoo, Shape design sensitivity analysis of a two-dimensional heat transfer system using the boundary element method, Computers and Structures 28 (1988) 543–550.
[8] K. Dems, Sensitivity analysis in thermal problems—II: structure shape variation, Journal of Thermal Stresses 10 (1987) 1–16.
[9] D.A. Tortorelli, R.B. Haber, S.C-Y. Lu, Design sensitivity analysis for nonlinear thermal systems, Computer Methods in Applied Mechanics and Engineering 77 (1989) 61–77.
[10] R.A. Meric, Boundary elements for static optimal heating of solids, Transactions of the ASME: Journal of Heat Transfer 106 (1984) 876–880.
[11] R.A. Meric, Shape design sensitivity analysis for nonlinear anisotropic heat conducting solids and shape optimization by the BEM, International Journal for Numerical Methods in Engineering 26 (1988) 109–120.
[12] S. Saigal, A. Chandra, Shape sensitivities and optimal configurations for heat diffusion problems: a beam approach, Transactions of the ASME, Journal of Heat Transfer 113 (1991) 287–295.
[13] P.Y. Shim, S. Manoochehri, Generating optimal configurations in structural design using simulated annealing, International Journal for Numerical Methods in Engineering 40 (1997) 1053–1069.
[14] Y.M. Xie, G.P. Steven, A simple evolutionary procedure for structural optimization, Computers & Structures 49 (1993) 885–896.
[15] Y.M. Xie, G.P. Steven, Evolutionary structural optimization for dynamic problems, Computers and Structures 58 (6) (1996) 1067–1073.
[16] Q. Li, G.P. Steven, O.M. Querin, Y.M. Xie, Topology design of structures subjected to thermal load by evolutionary optimization procedure, in: Proceedings of 1997 ASME Design Engineering Technical Conferences, DETC97DAC3974, Sacramento, USA, 1997.
[17] A. Bejan, Heat Transfer, John Wiley & Sons Inc., 1993.
[18] A. Sluzalec, M. Kleiber, Shape optimization of thermodiffusive systems, International Journal of Heat and Mass Transfer 35 (1992) 2299–2304.
[19] A.A. Seireg, J. Rodriguez, Optimizing the Shape of Mechanical Elements and Structures, Marcel Dekker Inc., New York, 1997.